ISSN: 2469-570X

Rieke et al. Int J Stem Cell Res Ther 2018, 5:051
DOI: 10.23937/2469-570X/1410051
Volume 5 | Issue 1
Open Access

International Journal of
Stem Cell Research & Therapy

ORIGINAL RESEARCH

Reconstructing Mammalian Retinal Tissue: Wnt3a Regulates Laminar Polarity in Retinal Spheroids from Neonatal Mongolian Rats, while RPE Promotes Cell Differentiation

Matthias Rieke, Afrim Bytyqi, Florian Frohns and Paul G Layer*

Entwicklungsbiologie & Neurogenetik, Technische Universität Darmstadt, Germany

***Corresponding author:** *Dr. Paul G Layer, Professor, Entwicklungsbiologie & Neurogenetik, Technische Universität Darmstadt, Schnittspahnstrasse 13, D-64287 Darmstadt, Germany, Tel: +6151-1624610, E-mail: layer@bio.tu-darmstadt.de*

Abstract

Besides invention of iPSC technology, recent progress of stem cell-based organoids is founded on long-standing 3D-reaggregate approaches from embryonic tissues. In particular, histotypic *in vitro* reconstruction of avian retinal spheroids was most prolific. For instance, a complete reconstitution of all retinal layers was possible, which was supported by Wnt signalling and factors from the retinal pigmented epithelium (RPE); similar *in vitro* findings are still missing for mammals. Using an established model of reaggregates from dispersed retinal cells of the neonatal Gerbil [1], we show here that in contrast to supernatant from RPE (RPE_{CM}), supplementation with Wnt3a induced a correct inside-out polarity of retinal layers. XAP1$^+$ precursors of photoreceptors (PRs) were correctly found on the external face of the sphere, but general cell differentiation remained limited. If Wnt3a was present for 4 days *in vitro* (div) only, the correctly polarized tissue further differentiated, e.g., more calretinin$^+$ amacrine cells (CR$^+$ ACs) sent out processes into an *ipl*-like layer and rhodopsin expression of PRs became detectable. Finally, if Wnt3a during 4 div was followed by RPE_{CM} treatment, all retinal layers with most cell types were arranged in correct order, as shown by markers including CR, Pax6, AChE, PKCá, CRALBP, and Cern901. LiCl experiments showed that the canonical Wnt/β-catenin pathway was involved. We conclude that Wnt3a conveyed a correct inside-out laminar polarity but kept cells in an undifferentiated state, while RPE_{CM} strongly promoted retinal differentiation. Both together supported a nearly complete retinal tissue reconstruction from fully dispersed cells, as never achieved before for cells from any mammalian retina.

Keywords

Gerbil, Inner plexiform layer, *Meriones unguiculatus*, Retinal spheroids, Retina tissue engineering, Retinal pigmented epithelium

Abbreviations

ACs: Amacrine Cells; AChE: Acetylcholinesterase; AM: Aggregation Medium; ATC: Acetylthiocholine; CMZ: Ciliary Marginal Zone; CM: Conditioned Medium; CR: Calretinin; dACs: Displaced Amacrine Cells; DAPI: 4',6-diamidine-2-phenylindole-dihydrochloride; div: Days *In Vitro*; DKK: Dickkopf; E: Embryonic Day; Fzd: Frizzled; GCL: Ganglion Cell Layer; GCs: Ganglion Cells; i.c.: In Culture; INL: Inner Nuclear Layer; IPL: Inner Plexiform Layer; HCs: Horizontal Cells; nbl: Neuroblastic Layer; ONL: Outer Nuclear Layer; OPL: Outer Plexiform Layer; P: Postnatal Day; PR: Photoreceptor; RPE: Retinal Pigmented Epithelium

Note: retinal layers in spheroids are denoted in lower-case letters, indicating that these are layers homologous, but not identical, to the *in vivo* retina.

Introduction

Tremendous progress has been made towards *in vitro* production of human organo-typic tissues, so-called *organoids* [2-5], since induced pluripotent stem cells (iPSCs) have become available from adult human tissues [6]. The possible applications of brain organoids, including retina, are widespread in transplantation medicine and pharmaceutical testing [7]. Besides the invention of iPSC production, organoid technologies are based on long-standing methods of histotypic reaggregation of embryonic stem cells from various tissue/organ origins. Reaggregation of completely dispersed retinal cells under constant rotation, and their differentiation into 3-dimensional histotypic retinal cell spheres (called *retinal spheroids*, or *retino-spheroids*) allow to

Citation: Rieke M, Bytyqi A, Frohns F, Layer PG (2018) Reconstructing Mammalian Retinal Tissue: Wnt3a Regulates Laminar Polarity in Retinal Spheroids from Neonatal Mongolian Rats, while RPE Promotes Cell Differentiation. Int J Stem Cell Res Ther 5:051. doi.org/10.23937/2469-570X/1410051

Received: February 27, 2018: **Accepted:** April 23, 2018: **Published:** April 25, 2018

analyse tissue construction in a "cell-by-cell" manner, and thus helps to develop rationales for the production of complete retinal tissues from appropriate embryonic or adult stem cells. Following primary reaggregation and sorting out of cells, periods of proliferation and differentiation of cells, and their correct integration into a 3D-tissue environment are formative. In fact, reaggregation of retinal and RPE cells from chicken embryos represented the most amenable and yielding model (reviewed in [8-10]). A first complete laminar retinal organisation has been achieved by mixing dissociated retinal pigmented epithelial (RPE) with retinal cells from the 5-6 days-old chicken embryo [11]. This model has allowed to analyse minute steps of retinal *in vitro* tissue formation (see Discussion); in fact, it let us predict the present progress in human regenerative medicine [8-10]. Until now, comparable histo-formative insights into differentiation of human retinal organoids from iPSCs have not yet been achieved.

Thus clearly, a detailed knowledge derived from avian and rodent reaggregate models can assist and direct progress of human organoid research. In contrast to avian retinal spheroids, however, in rodent (or any other mammalian) models a complete laminar retinal organisation had never been achieved [1,11,12]. Here, we have man-aged to produce highly laminar retinal spheroids from the neonatal Gerbil (Mongolian rat, or *Meriones unguiculatus*). In a previously established reaggregate model of retinal cells from the perinatal Gerbil [1], a first sign of histotypical organization was a circular arrangement of calretinin$^+$ amacrine cells, which had directed their processes into internal fibrous spaces, thus representing IPL-like areas (IPL: inner plexiform layer). Under the influence of supernatants from the RPE (RPE_{CM}), these "*ipl spaces*" began to fuse into a laminar ring below the surface of the sphere. The spheroids eventually reached a more coherent level of tissue organization, where most cell types were nicely arranged in cell layers, however, their inside-out orientation was inverted. Noticeably, photoreceptors (PRs) did not differentiate. Thus, the degree of self-organisation was remarkable, however, in contrast to the embryonic avian retina, RPE_{CM} alone was not capable of inducing a correct inside-out laminar order, and thus induce the reconstruction of an almost complete *in vitro* retina. Therefore, other factors and pathways originating from the retina itself had to be postulated to contribute to the formation of a complete retinal tissue.

Wnt signalling plays crucial roles in development, organisation and maintenance of many systems, including eye tissues [13-18]. Wnt2b was noted to inhibit differentiation of chicken retinal progenitor cells [19]. Wnt3, a close homologue to Wnt2b, is widely expressed in the pre- and postnatal mouse retina [20,21], and both, Wnt3 and Wnt2b, were reported to signal predominantly through the canonical Wnt/β-catenin pathway [19,22]. Clearly, activation of the canonical β-catenin pathway can strongly affect the acquisition of peripheral retinal characteristics both in chick and mouse [21,23]. Nevertheless, several studies have suggested that for neural retina development the canonical β-catenin pathway could be of minor significance. For mouse, Wnt/β-catenin signalling was associated with a non-canonical role [14]. Thereby, β-catenin activation was not affecting neurogenesis but rather retinal lamination, possibly by its functioning in cell adhesion [24].

In chick, the addition of Wnt2b to retinal reaggregates had induced their complete laminar organization [25], similar to what we had achieved in the avian system under the influence of supernatants from RPE or Müller cells [9,26-28]. Therefore, we here i) Not only found ways to produce laminar retinal spheroids from an embryonic mammal, but ii) Analysed the role(s) of Wnt3a in Gerbil retinal spheres, and correlated them with the effects of $RPE_{CM.}$ Expecting that both factors, Wnt3a and RPE, should exert similar effects, we found to the contrary that Wnt3a conveys the correct inside-out laminar arrangement, but delays further differentiation, while additional supplementation with RPE_{CM} is able to drive further differentiation within spheres. Thus, both components together are important synergistic regulators to achieve a nearly complete tissue organization of a rodent retina *in vitro*. How these findings can be instrumental in producing human retinal tissues from stem cells is briefly discussed.

Materials and Methods

Animals

Wildtype mongolian Gerbils (*Meriones unguiculatus*) were used throughout this study. Animal handling was performed according to approved national guidelines and the ARVO statement for animal care.

Retinal cell cultures

At least 14 retinae from newborn Gerbils (postnatal day 1; P1) were collected under sterile conditions in a hood. After decapitation, the eyes were isolated gently and collected in cold (4 °C) F-12 medium. The eye cups were opened by a micro-scissor along the *ora serrata*. Cornea, lens and vitreous body were removed. The eye cup was turned inside-out and each retina was carefully separated from the retinal pigment epithelium and from hyaloid vessels in order to avoid cellular contamination by non-retinal cells. After collecting the isolated retinas in F-12 medium on ice, the tissue was dissociated into completely dispersed cells as described before [1]. The retinal single cell preparation was seeded into 3.5 cm Petri dishes (~2.5×10^5 cells) in 2 ml aggregation medium (AM) and incubated for 10-12 days *in vitro*. The cell cultures were constantly rotated at 68 rpm on a flat gyratory shaker to produce reaggregated sphere cultures. Cells were cultured according to the following different experimental set-ups (*Experimental schemes* of Figure 1) in:

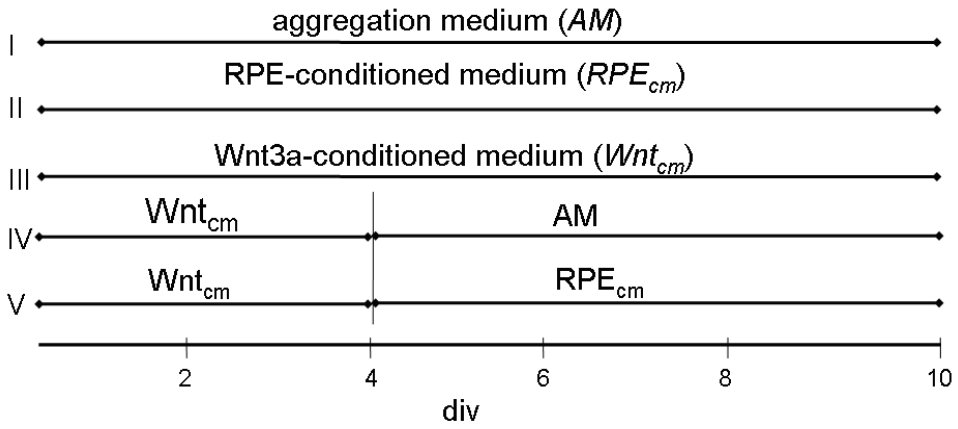

Figure 1: Schematic showing five different protocols for culturing dissociated cells from gerbil retina over a period of 10 days *in vitro* (div). Note that according to protocols IV and V, at div 4 Wnt_{cm} is replaced by aggregation medium (AM), or, by RPE supernatant (RPE_{cm}), respectively.

I. 2 ml aggregation medium (AM) for the whole period;

II. RPE_{CM} (see below) for the whole period;

III. $Wnt3a_{CM}$ (see below) for the whole period;

IV. For 4 days in $Wnt3a_{CM}$, followed by 6 days in AM;

V. For 4 days in $Wnt3a_{CM}$, followed by 6-8 days in RPE_{CM}.

AM (consisting of DMEM, 10% FCS, 1% L-glutamine, 0.1% penicillin, 0.02 mg/ml streptomycin) was changed every second day, while mixtures with conditioned media were replaced every 24 h.

RPE-conditioned medium - RPE_{CM}

For the production of RPE-conditioned media primary monolayer cultures from RPE were utilized. Eyes from P3 Gerbils were isolated and separated as above. The central parts of the eye cups were incubated in 1 ml dispase II (2.4 U/ml; Roche) plus 1 ml F12 medium for 10 min at 37 °C. The pigmented epithelium was isolated and collected in F12 medium on ice. Preparation of dissociated cells was as described before [1]. Cells from 3 eyes in 7 ml aggregation medium were seeded into 25 cm^2 laminin coated plastic flasks and incubated at 37 °C, 5% CO_2, 95% air. Medium was changed every 2nd day; cultures were kept for up to 24 days. After RPE cultures had reached confluency at about 10 days i.c., the medium was decanted and the dishes were replenished with 10 ml of fresh aggregation medium. After 3 days, the medium was collected, suspended cells were discarded and the supernatants (= RPE_{CM}) used directly or stored at -80 °C.

Wnt3a-conditioned medium - $Wnt3a_{CM}$

To produce Wnt3a-conditioned media, mouse L-M(TK-) fibroblasts secreting Wnt3a (ATCC CRL-2647), and non-transfected fibroblasts (ATCC CRL-2648) were cultured, following the protocol recommended by ATCC. Briefly, cells were grown on 15 cm^2 culture flasks (T15) nearly to confluency in DMEM supplemented with 10% FCS, 1% L-glutamine and 0.4 mg/ml of the antibiotic G-418 (Geneticin). After the medium was discarded, cells were washed with PBS, and medium replaced by 10 ml AM. The conditioned medium ($Wnt3a_{CM}$) was collected after 3 days and filtered.

LiCl treatment and β-catenin staining

Retinal cells from P1 Gerbils were isolated as described above and cultured for 48 h as monolayers on coverslips in a 3.5 cm Petri dish in 1 ml AM in presence of 15 mM LiCl or 15 mM NaCl for control. After washing and fixation, the cells were stained for β-catenin (1:1000; Sigma, Germany) and DAPI. Similarly, cells on coverslips were treated with $Wnt3a_{CM}$.

Determination of spheroid sizes

Average diameters of spheroids were determined from 20 spheres/time point, and average volumes of spheroids were calculated, using free accessible ImageJ software. The data set was compared by students t-test ($p \leq 0.1$).

Immunocytochemistry

After cultivation the retinal spheres were collected and gently sedimented (500 rpm/3 min). Fixation followed in 4% paraformaldehyde in PBS for 45 min at room temperature. The fixed spheres were soaked in 25% sucrose in PBS overnight at 4 °C. 10 µm-thick sections were cut on a cryostat (Microm, Heidelberg), and collected on gelatine-covered slides. The slides were dried and kept frozen until the staining process was started.

For immunocytochemical stainings, the sections were dried at 37 °C on a warming plate. Preincubation with 3% BSA/0.1% Triton-X-100 in PBS prevented unspecific binding, before sections were incubated with the primary antibodies overnight at 4 °C in a moist chamber. After two washing steps for 5 min with PBS, sections were incubated for 1 h with the second antibody, diluted in 1% Triton-X-100 in PBS. Again two washing steps in PBS followed. For additional nuclei staining, slides were incubated for 1 min with 100 µl DAPI solution (0.1 µg/ml),

before they were washed a third time for 10 min with PBS. After drying the slides on a warming plate, they were covered with Müllers Glycerin-Gelatine (Merck, Germany).

The primary and secondary antibodies and their working dilutions were as follows: Rabbit anti-CRALBP (1:600; Santa Cruz Biotechnology, INC), mouse anti-calretinin (1:1000; Swant, Bellinzona, Switzerland), rabbit anti-PKCá (1:300; Oxford Biomed. Res.), mouse anti-Pax6 (1:800; A. Kawakami, Biol. Sciences, University of Tokyo), rabbit anti-CERN901 (1:1000; Dr. W. de Grip, Nijmegen, Netherlands), mouse anti-XAP-1 (1:250; DSHB, Iowa), rabbit anti-β-catenin (1:1000; Sigma, Germany), Cy3-conjugated goat anti-mouse (1:100; Dianova, Hamburg, Germany), Cy3-conjugated goat anti-rabbit (1:100; Dianova, Hamburg, Germany), Cy2-conjugated goat anti-rabbit (1:100; Dianova, Hamburg, Germany).

Cholinesterase histochemistry

Acetylcholinesterase (AChE) activity was detected histochemically as previously described [28]. Substrate concentration was 2.4 mM for acetylthiocholine iodide (ATC) in presence of 100 µM tetraisopropyl pyrophosphoramide (iso-OMPA) to block butyrylcholinesterase. Incubation periods were 18-20 hours, at 37 °C in darkness. For negative controls, substrate was omitted, resulting in the absence of a brownish precipitate.

Microscopy and photography

Microscopy was performed on a ZEISS Axiophot (Jena, Germany), equipped with fluorescence and Nomarski optics, using 5-20x objectives and the appropriate fluorescence filters. Micrographs were taken by a digital INTAS 3-CCD camera (Intas, Göttingen, Germany) and stored with DISKUS 32 software package. Image editing and analyses were done by Adobe Photoshop 8.0 and Image J.

Results

The present findings are subdivided according to five different experimental schemes I-V (see Materials and Methods). In order to clearly demonstrate the progress achieved by schemes III-V (supplements of Wnt3a, or, Wnt3a + RPE_{cm}), basic results of schemes I (no supplements) and II (RPE_{cm} supplement) have to be briefly outlined (for more details see [1]).

Scheme I: Ground state of retinal tissue formation - ipl formation, but no lamination

Under treatment scheme I (no Wnt3a, no RPE supplements) the most basic degree of histotypic retinal tissue formation in Gerbil is achieved, which we here call the "*ipl_{space} ground state*" (cf. [1]). Dispersed cells (from P1 retina, in AM, no further supplements; see scheme I of Figure 1) from the neonatal Gerbil retina have the capacity to quickly reaggregate in full aggregation medium under rotation culture (see Figure 2a). Within a few days, a first sign of retinal tissue formation emerges by a circular arrangement of individual calretinin$^+$ amacrine cells (CR^+ ACs), occurring at several internal locations of the reaggregate (Figure 2a; cf. with calretinin staining of an *in vivo* retina in Figure 2e). These cells send out thick unipolar processes, all directed towards an inner neuropil-filled space; at its very centre, these processes amass and intermingle. In this system, a further laminar or otherwise differentiation was not observed.

Scheme II: RPE_{CM} promotes ipl differentiation and lamination, but not correct polarity

In the presence of a supernatant from RPE monolayer cultures (scheme II of Figure 1; Figure 2b and Figure 2c), besides a large ipl_{space} still in the centre of the sphere, many more ipl_{spaces} appeared near the surface of spheres and began to fuse with each other, to eventually transform into a contiguous laminar *ipl*, located closely under the outer surface (Figure 2b; within stippled circles). On each side of this *ipl*, CR^+ amacrine cells sent their processes into the *ipl*; often, these cells were arranged in pairs. Occasionally, bipolar and some horizontal cells were found internally, while rhodopsin expressing photoreceptors were missing (see for details [1]). Using the marker XAP-1, early photoreceptor precursors could be located at high numbers in the centre of this type of spheres (Figure 2c, scheme II). Therefore, the RPE_{CM} in this system promoted laminar differentiation within spheres, particularly acting on cells of the inner retina. However, the polarity of layers was inverted, e.g., a layer homologous to a GCL (furtheron called *gcl*; this does not mean to indicate that this is a complete GCL including all GCs) was outside with the other layers following towards the centre of the sphere (see further in Discussion).

Scheme III: Wnt3a conveys correct laminar polarity, but delays differentiation within spheres

In contrast to ipl_{space} spheres (Figure 2a) or RPE_{CM}-treated spheres (Figure 2b and Figure 2c), supplementation with Wnt3a induced spheroids with more coherently organised cells (scheme III of Figure 1; Figure 2d, Figure 2f and Figure 2g). In particular, DAPI-staining showed that cells of the outer half were forming a compact, organised mass, which began to separate from more loosely packed cells in the internal core (Figure 2d and Figure 2f). Thereby, open cell-free inner spaces were emerging (Figure 2d and Figure 2f). At the outer border of these cell-free spaces, a few individual CR^+ amacrine cells announced network formation of an *ipl* (in Figure 2d, *ipl* indicated by stippled circles). AChE staining independently supported the internal formation of an *ipl* in the internal part of the spheroid (Figure 2g). Individual $AChE^+$ cell bodies were similarly located along an internal ring, well corresponding with the ring of CR^+ amacrine cells (Figure 2g). Repeatedly, they appeared in a pairwise arrangement (arrows, Figure 2g), which is typical for cholinergic starburst amacrine cells of all vertebrate retinae [29-31]. Most importantly, however, XAP-1, a marker for early photoreceptor progenitor cells revealed strong

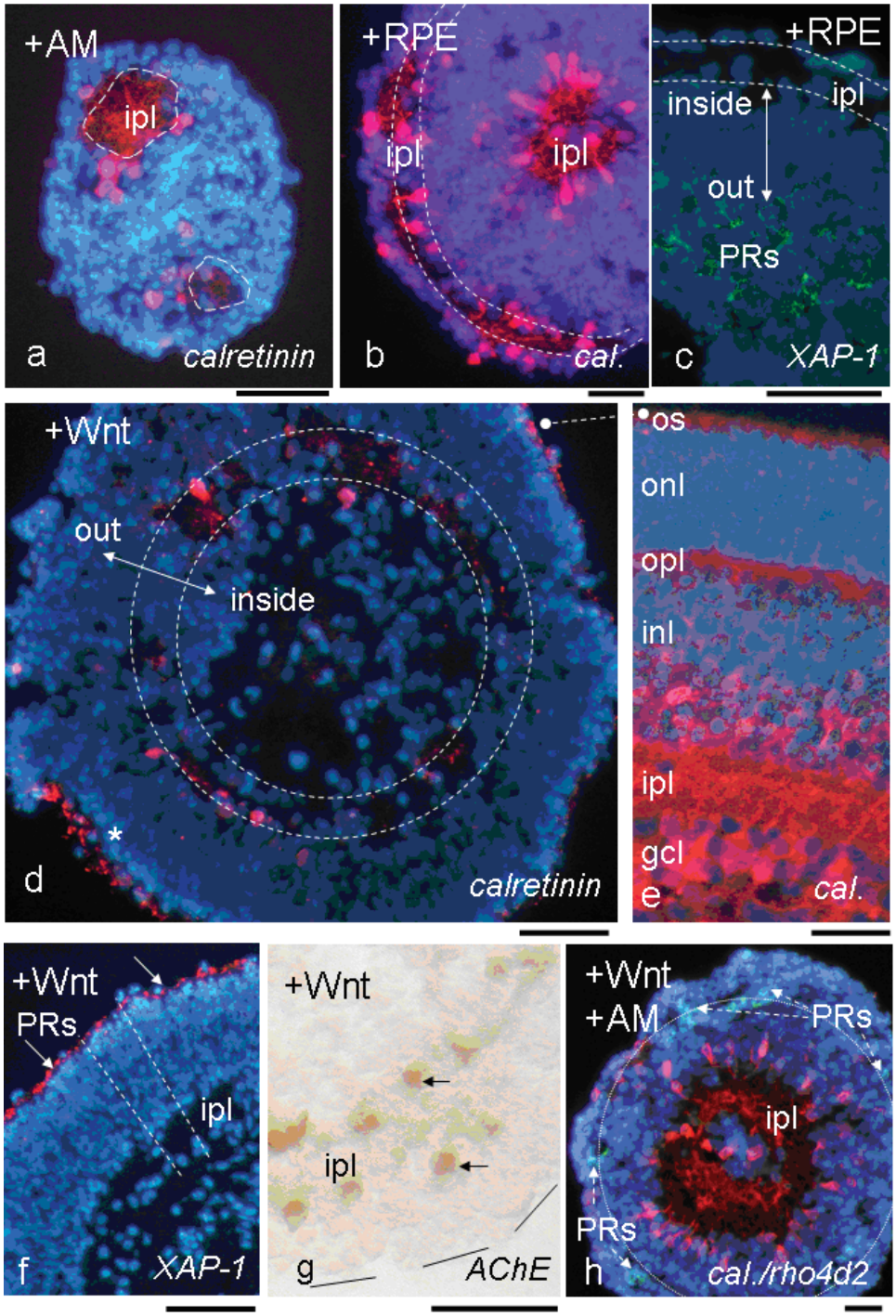

Figure 2: Distinct effects of treatment with Wnt3a (d, f, g) as compared with RPE_{CM} (b, c) on reaggregating cells from the perinatal Gerbil retina. In absence of both (a), in 10-days-old (10 div) spheroids, processes from circularly arranged calretinin$^+$ amacrine cells (CR^+ ACs; red) reach internally to form *ipl-like neuropil spaces* (see centres of a). In presence of RPE_{CM} (b; scheme II of Figure 1), a laminar *ipl* has formed near the sphere surface. XAP-1-stained PR precursors are located more to the center (c). In contrast, Wnt3a supplementation for 10 days (d, f, g; scheme III of Figure 1) induces a correct laminar inside-out polarity (double arrow in d; cf. with a section of a CR-stained P10 Gerbil retina in e). Compared with the control (a), DAPI in (d, f; blue) stains a compact ring of cells in the outer half sphere (note columnar arrangement of cells, dashed lines in f) with individual cells separating into a cell-free inner space (d, f). In (d) few CR^+ ACs are arranged in an inner ring (dashed double line). In (f), XAP-1 staining reveals photoreceptor precursors correctly located along the sphere surface. Formation of PR outer segments is announced by CR staining (star in d; cf. [32]). AChE staining further supports the internal location of the *ipl* (g); some of these cells appear pair-wise (arrows). In (h; scheme IV of Figure 1), a shorter Wnt3a exposure of only 4 div still induced a correct laminar polarity, and allowed further sphere differentiation. Compared with (d, f, g), many more CR^+ ACs extended their neurites into the *ipl* (red, dashed circle along inner *ipl* border); several PRs near the sphere surface are labelled by the rho4D2 antibody (green, arrows), where cell-free spaces announce formation of an *opl* (outer dashed line). Bars = 50 µm.

signals outside of the outermost DAPI-stained cell nuclei (arrows in Figure 2f), indicating the correct position of forming outer segments of PRs at the outermost rim of a future *onl*. This conclusion is further supported by CR staining at the sphere's periphery, outside of the most external cell bodies (star in Figure 2d), since CR stains

cone outer segments of PRs in adult Gerbil (own unpublished observations), and also of cat and human [32-34].

Scheme IV: Short Wnt3a and no RPE treatment - photoreceptors differentiate

If treatment with Wnt3a supernatant was restricted to the first 4 days i.c., to be then replaced by regular aggregation medium (AM, see scheme IV of Figure 1), many more CR$^+$ amacrine cells differentiated, surrounding an inner cell-free space (Figure 2h; cf. with Figure 2d). These CR$^+$ amacrine cells showed processes extending radially into the *ipl*; near the border at approximately 2/3 of *ipl* width towards a *gcl*-like cell layer, these processes extended laterally and heavily intermingled with each other. The spheroid centre was filled with cells, some of which were CR$^+$ cells. A cell-free ring emerged towards the surface of the sphere (stippled outer circle in Figure 2h), announcing the separation of the outer cell mass into *inl* and *onl*. In this region and only under scheme IV (not under scheme III), expression of rhodopsin became detectable in a few individual cells (green in Figure 2h, pinpointed by arrows), indicating progression of photoreceptor differentiation as compared with their precursor XAP-1$^+$ stage (see Figure 2f).

Therefore, when Wnt3a was present throughout the whole experiment, a correct in-side-out polarity of the whole retinal tissue was induced, with *gcl* and *ipl* forming inside, and an anlage of an *onl* with photoreceptor precursors outside. Differentiation of cells under these circumstances, however, appeared delayed. In contrast, when Wnt3a treatment was restricted to only 4 days (scheme IV) photoreceptor differentiation was advanced, further supporting our conclusions on Wnt3a actions.

Scheme V: RPE$_{CM}$ following Wnt3a treatment supports far-reaching differentiation of correctly laminated spheres

A further pronounced step of retinal tissue differentiation could be achieved under scheme V, e.g. 4 days treatment with Wnt3a to be followed by its replacement by RPE-conditioned medium (Figure 3b and Figure 3c). As a result, highly organised retinal spheres were produced at high rates, which presented all retinal layers, including a *gcl*, a wide *ipl*, an *inl*, an *opl* and an *onl* (Figure 3b and Figure 3c). These spheres resembled closely young developing mini-eyes, whereby the vitreous body was replaced in the centre of the spheres by a liquid-filled open space with a minor number of non-organised cells. A very high density of CR$^+$ amacrine cells and cells of the *gcl* bordered a wide *ipl*, which was filled by their intermingling neuropil. A dual *ipl* sublamination, as being typical for the *in vivo* retina (Figure 2e, Figure 3a and Figure 3b), sometimes began to emerge. Rhodopsin or opsin expressing photoreceptors now had become numerous. Depending on the particular spheroid, they had not yet found their final position (Figure 3b), or, a complete *onl* began to form with many photoreceptors being neatly arranged (Figure 3c, green). Additional markers were used to characterise retinal cell types and layers within the spheroid. PKCá labels a subset of bipolar cells, with cell bodies being located in the outer half of the INL; their radially oriented processes reach from the *opl* towards two wide layers of the *ipl* (Figure 4a; [35]). This pattern was also detected in spheroids (Figure 4b); most but not all cell bodies were in the right place (some were found at the outer rim of the *opl*). Their processes were running in parallel (but not as regularly as *in vivo*) from the *opl* into the *ipl*, where they seemed to amass near the inner border (not indicating two separate sublaminae) next to the *gcl*. Next, Müller cells with their radial processes throughout the retina as detected by CRALBP (Figure 4c) were present in high numbers in this type of spheroids (Figure 4d). Overlapping with CR staining, a Pax6 antibody stained many cells of the *gcl* and the inner *inl* (Figure 4f). Their density appeared somewhat lower than *in vivo* (cf. Figure 4e). The histochemical staining for AChE (Figure 4h; cf. Figure 4g for *in vivo* retina) presented two neuropil

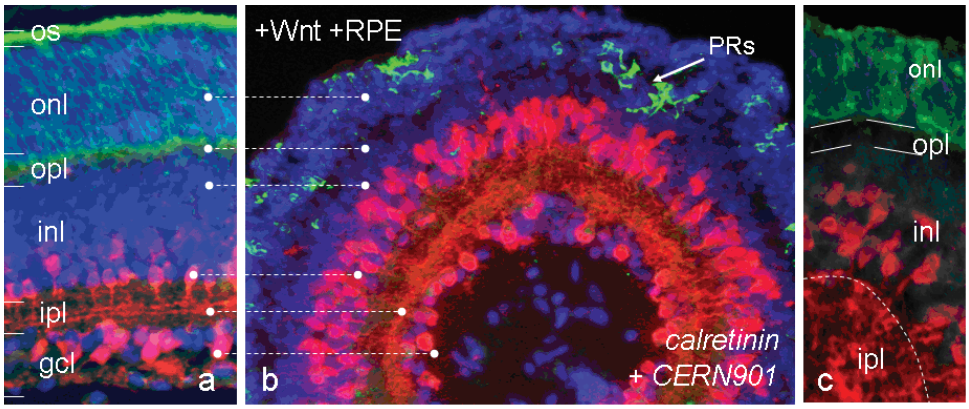

Figure 3: Optimal tissue formation after initial exposure to Wnt3a, followed by RPE supplementation (b; scheme V of Figure 1). After laminar polarity is established during 4 div in presence of Wnt3a, then RPE$_{CM}$ for further 6 div promotes strongly the differentiation into a fully laminated spheroid resembling closely a normal Gerbil retina (a). Numerous CR$^+$ ACs and their counterparts near the inner core send processes into the *ipl*, where they navigate laterally (red in b). Photoreceptors, as detected by CERN901 staining (green), are mostly correctly located outside of a cell-free *opl*-like ring (b, c). Their spatial organisation of 6-10 cell bodies within the *onl* and their degree of differentiation varies from spheroid to spheroid. Bar = 50 µm.

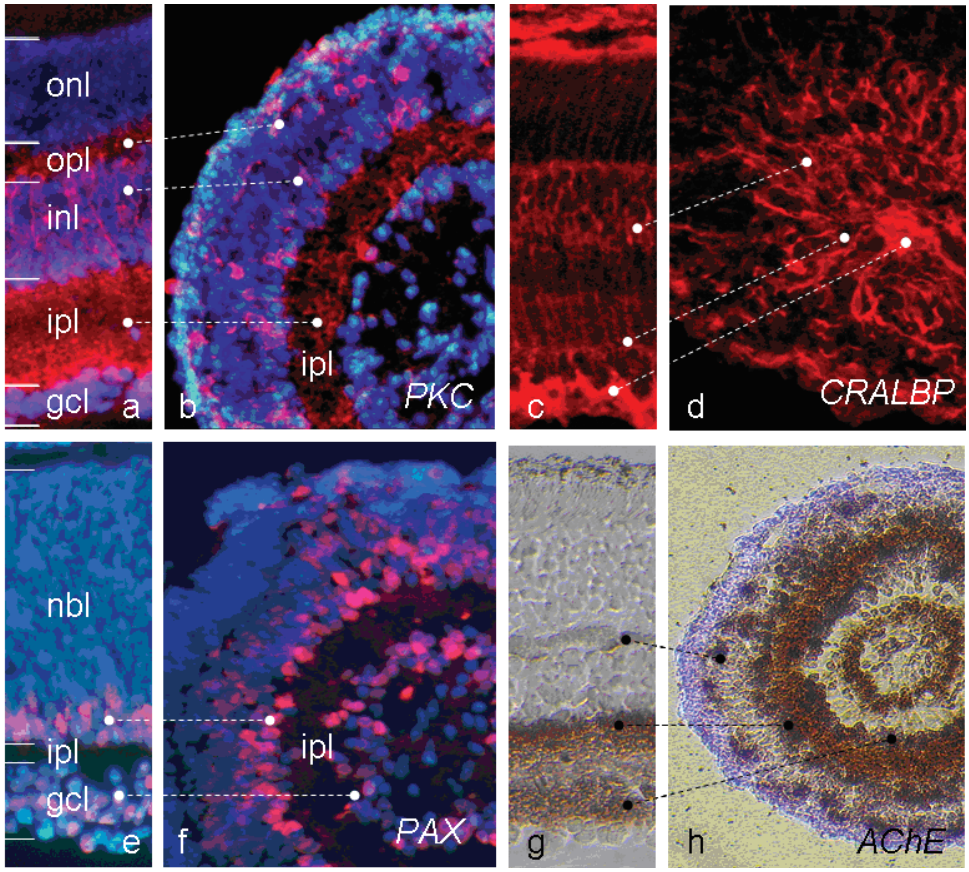

Figure 4: Complete laminar tissue differentiation after Wnt3a plus RPE treatment (scheme V), as characterised by specific cell markers. Comparing well with PKCα staining pattern for bipolar cells (BCs, red) in a P10 Gerbil retina (a), in a spheroid (b) BC somata are correctly located within the *inl*, with their processes reaching towards both plexiform layers. Note, only some BCs are dislocated in the outermost layer, Müller cells (MC) reach in parallel through the entire retina, as depicted by staining for CRALBP (c, red). In the spheroid shown in (d), radially oriented Müller cell processes are numerous. Their cell bodies are correctly located in the *inl*; their basal endfeet amass in the centre of the sphere. Pax6-staining of a spheroid section shows many stained amacrine cells on both sides of an internal *ipl* (f, red), comparable with their location in an adult Gerbil retina (e). AChE staining of a spheroid section (h) labels cells in *gcl*, in *inl* and their processes into the *ipl*; in addition horizontal cells (HCs) at regular distances with short processes into *opl* are stained. Staining compares well with *in vivo* staining (g). Bar = 50 µm.

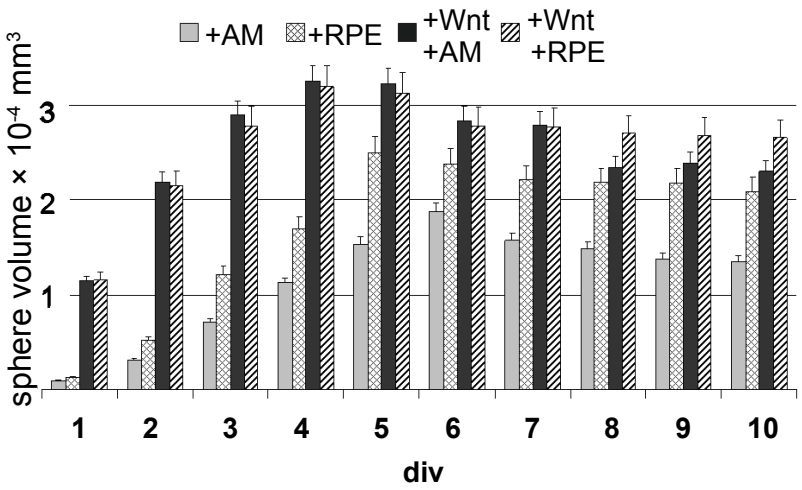

Figure 5: Spheroid volume growth under schemes I (AM control, light grey), II (RPE_{CM}, squared pattern), IV (Wnt_{CM} + AM, black) and V (Wnt_{CM} + RPE_{CM}, striped) is presented (since schemes III-V during the first 4 div are identical, scheme III is not shown). Note a strongly accelerated growth under Wnt_{CM} treatment. Sphere diameters have been determined from 20 spheres/time point; the data set was analysed by students t-test ($p \leq 0.1$; SD = 0.00065).

sublaminae within the *ipl* and their stained cell bodies in *inl* and *gcl*. Moreover, strongly stained individual cells were regularly spaced next to the *opl*. They appeared to be horizontal cells (HCs), which are known to express AChE during development [36-38], but normally at a lower activity (see further Discussion).

Wnt3a increases spheroid growth

From earlier studies it was known that after initial re-aggregation of dispersed retinal cells, the reaggregates grow quickly in size during the first 4-5 days i.c., due to a period of strong cell proliferation (Figure 5; [1]). In presence of RPE_{CM}, growth was significantly increased (scheme II, Figure 5, + RPE_{CM}). When comparing with both the AM-control and the RPE-spheres, the addition of Wnt3a promoted spheroid growth much more dramatically (Figure 5, +Wnt /+AM and +Wnt/+RPE_{CM}; note that during the first 4 days, scheme III, IV and V are identical, therefore scheme III is not shown here). The volumes of Wnt3a-supported spheres at div 1 were approx. 5-fold of AM-control. By div 5, Wnt3a-supported spheres were still approximately 50% larger than AM-controls, and 20% larger than RPE-spheres. After div 5, sphere sizes decreased in all samples by about 20%, due to cell death [1]. Clearly, Wnt3a promoted cell proliferation strongly, which certainly contributed to its distinct effects during spheroid lamination and differentiation.

Wnt3a acts through the canonical Wnt/β-catenin pathway

Normally, Wnt3a ligands act through the canonical Wnt pathway, and so did Wnt3a in our experiments. Thereby, dishevelled inhibits GSK-3β; as a consequence β-catenin is transferred from the cytoplasm to the nucleus. When we raised cells from P1 Gerbil retina in monolayer culture in control medium (AM), their cytoplasm presented a diffuse distribution of β-catenin, while the nuclei remained mostly spared (Figure 6a and Figure 6b, control). However, when treated with 15 mM LiCl, β-catenin was strongly accumulating in nuclei (Figure 6c and Figure 6d), showing that our cells were able to use the canonical pathway. Moreover, supernatants from Wnt3a-secreting L-M (TK-) fibroblasts did exert the same effect (Figure 6e and Figure 6f), proving that the Wnt3a-supernatant used in this study could activate the β-catenin pathway in Gerbil retinal cells. Not only in monolayer culture, but also during 3D-spheroid formation was this same pathway active, as shown by the correctly polarised spheres. When retinal reaggregates from P1 Gerbil were grown in presence of 15 mM LiCl, their structure was comparable with results as achieved in presence of Wnt3a (Figure 6g; cf. scheme III, Figure 2d, Figure 2f), e.g. a correct in-side-outside laminar organisation, whereby the *ipl* began to form inside and the first PR precursors were located towards the surface of the sphere. This proves that Wnt3a exerted its effects via the canonical Wnt/β-catenin pathway.

Discussion

This study provides distinct answers on how Wnt3a and RPE-secreted factors regulate basic processes of retinal tissue formation in three-dimensional retinal re-aggregates from newborn gerbils. Originally, the Gerbil retina had been chosen for its larger eye size, its delayed differentiation at birth and its higher rate of cones, as com-pared with mouse or rat [1]. The present study demonstrated that Gerbil retinal cells can be brought to a higher degree of retinal tissue reconstruction than

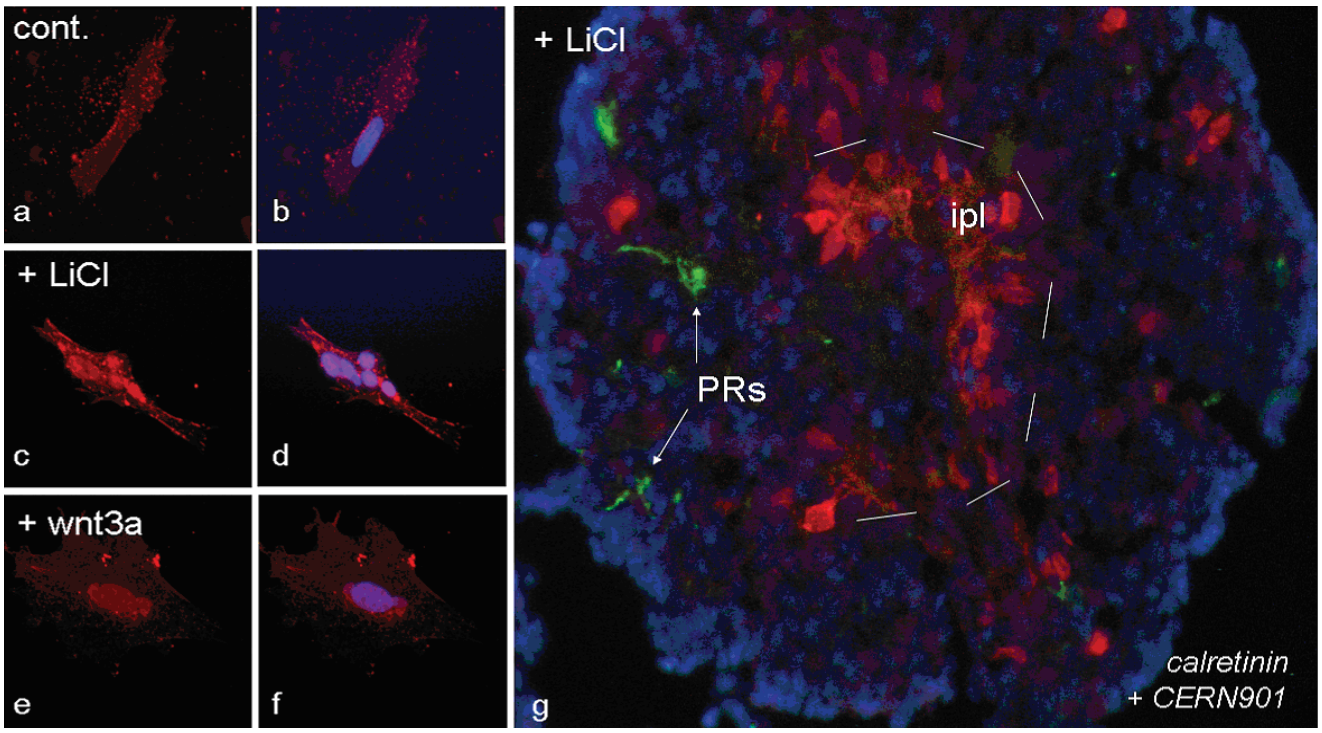

Figure 6: Both, Wnt3a and LiCl activate the canonical Wnt pathway in P1 Gerbil monolayer retinal cells (a-f), and in retinal 3D spheroids (g). Note translocation of β-catenin (red) into nucleus after Wnt3a (e, f) and LiCl treatment (c, d), while in control β-catenin remains outside of nucleus of retinal cells (a, b). In presence of LiCl, spheres grow very large with a structure similar to that of spheres treated with Wnt3a (scheme III of Figure 1), with an *ipl* forming inside (dashed line) and a few photoreceptors towards outside (green; cf. Figure 3). Bar in (a-f) = 12.5 µm, (g) = 25 µm.

ever achieved before with any other rodent cells. This progress will be instrumental to advance applicabilities of not only rodent, but eventually also human organoid technologies, as has been shown by avian retinal spheroid technologies. Their high reproducibility of spheroid formation rendered them applicable as developmental assay systems to analyse genetic (by gene knockout) or molecular (environmental) effects on tissue development, e.g., by growth factors or environmental stress. Histologic changes of spheroids became easily tractable by applying simple phase contrast microscopy of whole spheroids in combination with isocontour imaging using Image-J software [39,40]. Moreover, retinal spheroids were introduced for automated high-throughput pharmacological and electrophysiological analyses (cf. [41-43]).

Wnt signaling is involved in tissue lamination

Through analysis of retinogenesis in retinal reaggregates from chicken embryonic retinae, we had succeeded to convert a rosetted spheroid type into a completely laminar type of sphere by secreted factors from RPE cells, from cells of the ciliary margin (CMZ) or from isolated Müller cells [26,27,38]. Another group had found that Wnt2b precisely could mimic this effect [25], and therefore Wnt2b promised to represent *the* relevant tissue-forming factor from CMZ, RPE, or Müller cells. By turning to a mammalian retinal reaggregate system, we were hoping to find further support for this assumption. In chick, Wnt2b at the CMZ inhibited differentiation of retinal progenitors via the canonical Wnt pathway (and via LEF) [19,23,44]. For mammals, the role of the Wnt pathway remains uncertain, although an Frz5 receptor is expressed in the CMZ. Our results revealed much novel information; in particular in presence of RPE plus Wnt3a (scheme V) an optimal tissue reconstruction was achieved for the first time from a mammalian retina. Thereby, all retinal layers were established in correct inside-out sequence, and cellular differentiation reached a far-advanced degree. Such a complete retinal tissue reconstruction from completely dispersed cells has not been achieved for any mammalian retina before.

Wnt3a stabilizes the undifferentiated state, while RPE promotes differentiation

We here used Wnt3a as a promising surrogate for Wnt2b, since Wnt3a is already expressed in the eye *anlage* [45], and supported retinal regeneration in a lesioned adult mouse retina through the Wnt/β-catenin pathway [46]. Therefore, Wnt3a appeared to be a most relevant factor for early retinal tissue formation. Besides controlling the correct polarity of retinal tissue, another feature of Wnt3a action - and more pronounced than in presence of RPE - was that it led to a massive increase of cell numbers and thus to a rapid increase of spheroid size. Cells of Wnt3a-supported spheroids resembled an organised mass of progenitors, where differentiation was slowed (or even halted), e.g., CR^+ amacrine cells remained at low numbers. Photoreceptor progenitors were placed at the right position, but remained in a precursor state. Therefore, it is likely that Wnt3a has a role only during very early retinogenesis, while in adult Gerbil retina its expression disappears (data not shown). This is reminiscent of the role assigned to Wnt2b in the chick CMZ [19,45]. That Wnt3a kept cells in an undifferentiated state was further supported by our scheme IV experiments, where $Wnt3a_{CM}$ was supplemented only for the first 4 div (Figure 2h). After removal of the Wnt ligand, differentiation proceeded, with appearance of more CR^+ cells and formation of an *opl*; even PRs began to express rhodopsin. This conclusion corresponds with reports that Wnt signalling regulates various stem cell populations [47,48]. Accordingly, mouse embryonic stem cells treated at early stages with Wnt and Nodal antagonists (Dkk1 and LeftyA) strongly supported neural differentiation [49].

For chick retinal reaggregates, it had been suggested that Wnt2b not only can simulate the effect of RPE, but it may represent *the active factor* within the RPE supernatant [25]. Here, with a rodent system, the action of RPE_{CM} was clearly distinct from that of Wnt3a. RPE_{CM} promoted proliferation only to a minor degree. Instead, the main action of RPE was an acceleration of differentiation, promoting cells of the inner retina (CR^+ ACs) to form a contiguous *ipl*, but also it pushed PRs into premature differentiation (Figure 3b and Figure 3c), which in absence of RPE (scheme I) did not occur from P1 cells, and only would emerge in AM cultures from P3 retinae (not shown; [1]). The molecular nature of the active RPE factor(s) remains unclear, including several candidates [50,51].

It appears that both Wnt3a and RPE supplementations acted together in a balanced way: If Wnt3a acted alone, an undifferentiated state was stabilized and the tissue polarized correctly, but its further differentiation remained halted. On the other side, if RPE acted alone, differentiation of the tissue was speeded up (too) much, so that a correct inside-outside polarisation of layers could not be established. A series of cell type- and lamina-specific staining procedures supported these findings (Figure 4), showing that most major cell types of the retina were expressed and located correctly within the tissue (cf. [1]). AChE histochemistry, by revealing a dual sublamination within the IPL in some of the spheres, indicates a most advanced state of *ipl* differentiation with ON and OFF sublayers [28]. Synapse-specific SV-2 expression showed that network formation in the *ipl* even reached synaptogenesis (data not shown).

Conclusions

Our 3D-retinal spheroid models enabled us to show that Wnt3a has an entirely different function compared with RPE, and that both components act sequentially together to trigger formation of an almost complete mammalian retinal tissue. Although production and handling

of 3-dimensional cellular spheres is time-consuming and imaging is still difficult [52], the overwhelming progress of stem cell biology would not have been possible without going 3-dimensional [7]. This study underscores once again that spheroid technologies allow to decipher step-by-step not only the formation of a retina. Such knowledge is most useful in developing biomedical applications, e.g., reconstruction of retinal tissue from appropriate animal or human stem cells [2-5,42,53-55], or, for development of living biosensors on cell chips as pharmaceutical drug assay systems [7,41,43].

Acknowledgements

We thank A.H. Bytyqi, L. Wright, L.E. Sperling, A. Vogel-Höpker and E. Willbold for helpful discussions. We acknowledge the expert technical assistance by J. Huhn, M. Stotz-Reimers and K. Wehner. This work was supported by the Deutsche For-schungsgemeinschaft (DFG, La 379/12-4).

Conflict of Interests

None.

References

1. Bytyqi AH, Bachmann G, Rieke M, Paraoanu LE, Layer PG (2007) Cell-by-cell reconstruction in reaggregates from neonatal gerbil retina begins from the inner retina and is promoted by retinal pigmented epithelium. Eur J Neurosci 26: 1560-1574.
2. Meyer JS, Shearer RL, Capowski EE, Wright LS, Wallace KA, et al. (2009) Modeling early retinal development with human embryonic and induced pluripotent stem cells. Proc Natl Acad Sci USA 106: 16698-16703.
3. Eiraku M, Takata N, Ishibashi H, Kawada M, Sakakura E, et al. (2011) Self-organizing optic-cup morphogenesis in three-dimensional culture. Nature 472: 51-56.
4. Lancaster MA, Renner M, Martin CA, Wenzel D, Bicknell LS, et al. (2013) Cerebral organoids model human brain development and microcephaly. Nature 501: 373-379.
5. Zhong X, Gutierrez C, Xue T, Hampton C, Vergara MN, et al. (2014) Generation of three-dimensional retinal tissue with functional photoreceptors from human iPSCs. Nat Commun 5: 4047.
6. Takahashi K, Yamanaka S (2006) Induction of pluripotent stem cells from mouse embryonic and adult fibroblast cultures by defined factors. Cell 126: 663-676.
7. Huch M, Knoblich JA, Lutolf MP, Martinez-Arias A (2017) The hope and the hype of organoid research. Development 144: 938-941.
8. Layer PG, Willbold E (1994) Regeneration of the avian retina by retinospheroid technology. Prog Ret Res 13: 197-230.
9. Layer PG, Rothermel A, Willbold E (2001) From stem cells towards neural layers: A lesson from re-aggregated embryonic retinal cells. Neuroreport 12: 39-46.
10. Layer PG, Robitzki A, Rothermel A, Willbold E (2002) Of layers and spheres: The reaggregate approach in tissue engineering. Trends Neurosci 25: 131-134.
11. Akagawa K, Hicks D, Barnstable CJ (1987) Histiotypic organization and cell differentiation in rat retinal reaggregate cultures. Brain Res 437: 298-308.
12. Watanabe T, Voyvodic JT, Chan-Ling T, Sagara H, Hirosawa K, et al. (1997) Differentiation and morphogenesis in pellet cultures of developing rat retinal cells. J Comp Neurol 377: 341-350.
13. Megason SG, McMahon AP (2002) A mitogen gradient of dorsal midline Wnts organizes growth in the CNS. Development 129: 2087-2098.
14. Fuhrmann S, Stark MR, Heller S (2003) Expression of Frizzled genes in the developing chick eye. Gene Expr Patterns 3: 659-662.
15. Nusse R (2005) Wnt signaling in disease and in development. Cell Res 15: 28-32.
16. Van Raay TJ, Vetter ML (2004) Wnt/frizzled signaling during vertebrate retinal development. Dev Neurosci 26: 352-358.
17. Steinfeld J, Steinfeld I, Coronato N, Hampel ML, Layer PG, et al. (2013) RPE specification in the chick is mediated by surface ectoderm-derived BMP and Wnt signalling. Development 140: 4959-4969.
18. Steinfeld J, Steinfeld I, Bausch A, Coronato N, Hampel ML, et al. (2017) BMP-induced reprogramming of the neural retina into retinal pigment epithelium requires Wnt signalling. Biol Open 6: 979-992.
19. Kubo F, Takeichi M, Nakagawa S (2003) Wnt2b controls retinal cell differentiation at the ciliary marginal zone. Development 130: 587-598.
20. Fevr T, Robine S, Louvard D, Huelsken J (2007) Wnt/beta-catenin is essential for intestinal homeostasis and maintenance of intestinal stem cells. Mol Cell Biol 27: 7551-7559.
21. Liu H, Xu S, Wang Y, Mazerolle C, Thurig S, et al. (2007) Ciliary margin transdifferentiation from neural retina is controlled by canonical Wnt signaling. Dev Biol 308: 54-67.
22. Liu H, Mohamed O, Dufort D, Wallace VA (2003) Characterization of Wnt signaling components and activation of the Wnt canonical pathway in the murine retina. Dev Dyn 227: 323-334.
23. Cho SH, Cepko CL (2006) Wnt2b/beta-catenin-mediated canonical Wnt signaling determines the peripheral fates of the chick eye. Development 133: 3167-3177.
24. Fu X, Sun H, Klein WH, Mu X (2006) Beta-catenin is essential for lamination but not neurogenesis in mouse retinal development. Dev Biol 299: 424-437.
25. Nakagawa S, Takada S, Takada R, Takeichi M (2003) Identification of the laminar-inducing factor: Wnt-signal from the anterior rim induces correct laminar formation of the neural retina in vitro. Dev Biol 260: 414-425.
26. Rothermel A, Willbold E, Degrip WJ, Layer PG (1997) Pigmented epithelium induces complete retinal reconstitution from dispersed embryonic chick retinae in reaggregation culture. Proc Biol Sci 264: 1293-1302.
27. Willbold E, Rothermel A, Tomlinson S, Layer PG (2000) Muller glia cells reorganize reaggregating chicken retinal cells into correctly laminated in vitro retinae. Glia 29: 45-57.
28. Layer PG, Berger J, Kinkl N (1997) Cholinesterases precede “ON-OFF” channel dichotomy in the embryonic chick retina before onset of synaptogenesis. Cell Tissue Res 288: 407-416.
29. Tauchi M, Masland RH (1984) The shape and arrangement of the cholinergic neurons in the rabbit retina. Proc R Soc Lond B Biol Sci 223: 101-119.
30. Greferath U, Grunert U, Mohler H, Wassle H (1993) Cholinergic amacrine cells of the rat retina express the delta-subunit of the GABAA-receptor. Neurosci Lett 163: 71-73.

31. Prada F, Medina JI, Lopez-Gallardo M, Lopez R, Quesada A, et al. (1999) Spatiotemporal gradients of differentiation of chick retina types I and II cholinergic cells: Identification of a common postmitotic cell population. J Comp Neurol 410: 457-466.

32. Goebel DJ, Pourcho RG (1997) Calretinin in the cat retina: Colocalizations with other calcium-binding proteins, GABA and glycine. Vis Neurosci 14: 311-322.

33. Nag TC, Wadhwa S (1999) Developmental expression of calretinin immunoreactivity in the human retina and a comparison with two other EF-hand calcium binding proteins. Neuroscience 91: 41-50.

34. Pasteels B, Rogers J, Blachier F, Pochet R (1990) Calbindin and calretinin localization in retina from different species. Vis Neurosci 5: 1-16.

35. Haverkamp S, Haeseleer F, Hendrickson A (2003) A comparison of immunocytochemical markers to identify bipolar cell types in human and monkey retina. Vis Neurosci 20: 589-600.

36. Hutchins JB, Bernanke JM, Jefferson VE (1995) Acetylcholinesterase in the developing ferret retina. Exp Eye Res 60: 113-125.

37. Kim IB, Park DK, Oh SJ, Chun MH (1998) Horizontal cells of the rat retina show choline acetyltransferase- and vesicular acetylcholine transporter-like immuno-reactivities during early postnatal developmental stages. Neurosci Lett 253: 83-86.

38. Layer PG, Willbold E (1989) Embryonic chicken retinal cells can regenerate all cell layers in vitro, but ciliary pigmented cells induce their correct polarity. Cell Tissue Res 258: 233-242.

39. Frohns F, Mager M, Layer PG (2009) Basic fibroblast growth factor increases the precursor pool of photoreceptors, but inhibits their differentiation and apoptosis in chicken retinal reaggregates. Eur J Neurosci 29: 1931-1942.

40. Eldred MK, Muresan L, Harris WA (2017) Disaggregation and reaggregation of zebrafish retinal cells for the analysis of neuronal layering. Methods Mol Biol.

41. Rothermel A, Biedermann T, Weigel W, Kurz R, Ruffer M, et al. (2005) Artificial design of three-dimensional retina-like tissue from dissociated cells of the mammalian retina by rotation-mediated cell aggregation. Tissue Eng 11: 1749-1756.

42. Daus AW, Layer PG, Thielemann C (2012) A spheroid-based biosensor for the label-free detection of drug-induced field potential alterations. Sensors and Actuators B: Chemical 165: 53-58.

43. Rieke M, Gottwald E, Weibezahn KF, Layer PG (2008) Tissue reconstruction in 3D-spheroids from rodent retina in a motion-free, bioreactor-based microstructure. Lab Chip 8: 2206-2213.

44. Kubo F, Takeichi M, Nakagawa S (2005) Wnt2b inhibits differentiation of retinal progenitor cells in the absence of Notch activity by downregulating the expression of proneural genes. Development 132: 2759-2770.

45. Inoue T, Kagawa T, Fukushima M, Shimizu T, Yoshinaga Y, et al. (2006) Activation of canonical Wnt pathway promotes proliferation of retinal stem cells derived from adult mouse ciliary margin. Stem Cells 24: 95-104.

46. Nasrallah I, Golden JA (2001) Brain, eye, and face defects as a result of ectopic localization of Sonic hedgehog protein in the developing rostral neural tube. Teratology 64: 107-113.

47. Reya T, Duncan AW, Ailles L, Domen J, Scherer DC, et al. (2003) A role for Wnt signalling in self-renewal of haematopoietic stem cells. Nature 423: 409-414.

48. Otero JJ, Fu W, Kan L, Cuadra AE, Kessler JA (2004) Beta-catenin signaling is required for neural differentiation of embryonic stem cells. Development 131: 3545-3557.

49. Watanabe K, Kamiya D, Nishiyama A, Katayama T, Nozaki S, et al. (2005) Directed differentiation of telencephalic precursors from embryonic stem cells. Nat Neurosci 8: 288-296.

50. Esteve P, Trousse F, Rodriguez J, Bovolenta P (2003) SFRP1 modulates retina cell differentiation through a beta-catenin-independent mechanism. J Cell Sci 116: 2471-2481.

51. Araki M (2007) Regeneration of the amphibian retina: Role of tissue interaction and related signaling molecules on RPE transdifferentiation. Dev Growth Differ 49: 109-120.

52. Pampaloni F, Reynaud EG, Stelzer EH (2007) The third dimension bridges the gap between cell culture and live tissue. Nat Rev Mol Cell Biol 8: 839-845.

53. Gamm DM, Wang S, Lu B, Girman S, Holmes T, et al. (2007) Protection of visual functions by human neural progenitors in a rat model of retinal disease. PLoS One 2: e338.

54. Lamba D, Karl M, Reh T (2008) Neural regeneration and cell replacement: A view from the eye. Cell Stem Cell 2: 538-549.

55. Osakada F, Ikeda H, Mandai M, Wataya T, Watanabe K, et al. (2008) Toward the generation of rod and cone photoreceptors from mouse, monkey and human embryonic stem cells. Nat Biotechnol 26: 215-224.